Nitric Oxide 83 (2019) 24–32

Contents lists available at ScienceDirect

Nitric Oxide

journal homepage: www.elsevier.com/locate/yniox

Is it possible to combine photodynamic therapy and application of dinitrosyl iron complexes in the wound treatment?

Anna B. Solovieva[a], Anatoly F. Vanin[a,b], Anatoly B. Shekhter[b], Nikolay N. Glagolev[a], Nadezhda A. Aksenova[a,b], Vasak D. Mikoyan[a], Svetlana L. Kotova[a,b,*], Tatyana G. Rudenko[b], Alexey L. Fayzullin[b], Peter S. Timashev[a,b,c]

[a] Department of Polymers and Composites, N.N.Semenov Institute of Chemical Physics, RAS, 4 Kosygin St., Moscow, 119991, Russia
[b] Institute for Regenerative Medicine, Sechenov University, 8-2 Trubetskaya St., Moscow, 119991, Russia
[c] Institute of Photonic Technologies, Research Center "Crystallography and Photonics", RAS, 2 Pionerskaya st., Troitsk, Moscow, 142190, Russia

ARTICLE INFO

Keywords:
Dinitrosyl iron complexes
Nitric oxide
Photodynamic therapy
Chlorines
Amphiphilic polymers
Pluronics

ABSTRACT

We have studied the effect of interactions between dinitrosyl iron complexes with thiol-containing ligands (DNIC-TL) and diglucamine salt of chlorine e6 (photoditazine, PD) on the rate of photosensitized oxidation of a model organic substrate – tryptophan – in the presence and absence of an amphiphilic polymer, Pluronic F127, as well as on the DNIC-TL and PD photostability. Using EPR and UV spectroscopy, we determined the rate constants for photodegradation of mono- and dinuclear DNIC-TL and PD, respectively. The presence of the photosensitizer and Pluronic F127 has been shown to have a negligible effect on the rate of photodestruction of mono- and dinuclear DNIC-TL, taking into account the changing DNIC-TL and PD concentrations in the photoexcitation conditions. At the same time, in the DNIC-TL presence, the rate of PD photodestruction increases, however, addition of Pluronic F127 leads to a decrease in the rate constant of PD photodestruction. The latter circumstance creates an opportunity for a simultaneous application of DNIC-TL and photodynamic therapy in the wound treatment without losing the PDT efficiency. Indeed, photodynamic therapy in combination with DNIC-TL facilitated skin wound healing in laboratory rats. As shown by a morphological study, application of the DNIC-TL-PD-F127 complex with the subsequent photoactivation was beneficial in reducing inflammation and stimulating regenerative processes.

1. Introduction

The interest to short-living biologically active simple molecules, in particular, to nitric oxide and reactive oxygen species (ROS) arises from the fact that such substances perform a function of regulators at different levels of live species organization [1,2]. Nitric oxide is a multifunctional signal molecule which controls intra- and intercellular processes in animal, bacterial and plant organisms and provides both promoting (regulatory, protective) and inhibiting effects on the metabolism [3–6]. In particular, the radical form $NO^{\cdot}$ plays a crucial role in the functioning of immune, nervous systems in animals, in growth and development of plants [7–9]. The small size and absence of a charge stipulate high penetration of nitric oxide molecules through cell membranes and those of subcell structures. The characteristic lifetime of nitric oxide in biological tissues may vary substantially. For example, in the renal tissue of rats it equals 6.4 s, in the myocardium– 0.1 s, in the blood – (0.05–0.2) s, while in water, from which oxygen was removed, NO molecules are preserved for several days. Therefore, nitric oxide is a perfect carrier during short-time auto- or paracrine cell signal exchange. In turn, ROS are necessary components of the cell life activity and of an organism as a whole [10,11] and in fact comprise a separate system in a body, participating both in a number of physiological functions and in many pathological processes. The most important ROS are superoxide radical $\dot{O}^{-}$, singlet oxygen $^1O_2$, hydroxyl $O\dot{H}$ and peroxide $H\dot{O}_2$ radicals, hydrogen peroxide H_2O_2, peroxide ion HO_2^{-}, hypochlorite *HOCl*. The average ROS concentration in human tissues is 8–10 mM [10]. ROS actively participate in the processes of intracell signal transfer that is important for the normal cell growth [11]. It is the creation of high ROS concentrations exceeding the average values that is the characteristic function of so-called professional phagocytes – cells of congenital immunity [12]. Lower ROS concentrations are constantly present in almost all the cells of a body and they perform the signal functions as secondary intermediates in redox-sensitive signal pathways [13,14]. Thus, ROS are universal regulatory agents in plant and animal

* Corresponding author. Department of Polymers and Composites, N.N.Semenov Institute of Chemical Physics, RAS, 4 Kosygin St., Moscow, 119991, Russia.
E-mail address: slkotova@mail.ru (S.L. Kotova).

https://doi.org/10.1016/j.niox.2018.12.004
Received 30 July 2018; Received in revised form 1 November 2018; Accepted 9 December 2018
Available online 14 December 2018
1089-8603/

organisms [15,16], favorably affecting the life activity processes from the cell level up to the whole body level.

It has currently been established that the reactive oxygen and nitrogen species participate in the development of pathologies related to the oxidative stress, including atherosclerosis, ischemic heart disease, neurodegenerative diseases, cataract, cancer, diabetes. Besides, interaction of nitric oxide and its derivatives with ROS results in the formation of reactive metabolites of nitric oxygen – peroxynitrite, nitric dioxide, NO_2Cl, which are important components of the immune response in human and animal organisms [17–20]. Among the processes of such a type, the ROS interaction with dinitrosyl iron complexes with thiol-containing ligands (DNIC-TL) has been studied most intensively, since such complexes are capable of playing a role of donors of $NO^{\cdot}$ and NO^{+} in biosystems and controlling not only cytotoxic, but also regulatory-regenerative processes [21].

In spite of the importance of these processes for an organism, the mechanisms of ROS interactions with nitric oxide and some of its derivatives, including DNIC-TL, are still poorly studied [22]. In particular, the literature sources describe singlet oxygen quenching resulting from its interaction with methyl-substituted nitrosopropane and trimethyl-substituted nitrosomethane in an ethanol-methylene chloride mixture [23], as well as from its interaction with S-nitrosoglutathione. In the latter case, singlet oxygen was obtained by means of photoexcitation of some photosensitizers (rose bengal, hematoporphyrin) [24]. Photooxidation of nitrosoalkanes and nitrosocycloalkanes in organic solvents (benzene, chloroform, methanol) to the corresponding nitrates has also been studied [25]. However, many issues still remain unsolved, concerning the mechanism of DNIC-TL decomposition and a possibility of controlled exterior influence on the biological activity of DNIC-TL. In this connection, photostimulated and photosensitizing effects on the DNIC-TL decomposition with generation of $NO^{\cdot}$ radicals are of primary interest [26].

Since ROS photogeneration represents a basis for oxidative destruction of pathological cells and tissues (malignant and benign tumors, purulent wounds, trophic ulcers) upon photoexcitation of a photosensitizer administered to a lesion (photodynamic therapy, PDT), a new possibility arises for the search of PDT combination with the DNIC-TL action. In other words, one may consider a combination of a relatively “mild” destructive photodynamic action with the simultaneous photoinitiation of regulatory-regenerative processes due to decomposition of DNIC-TL accompanied by appearance of $NO^{\cdot}$ radicals in the reaction medium.

This article is dedicated to the consideration of some aspects of nitric oxide interaction with photodynamic agents. We analyze a possibility of the simultaneous application of singlet oxygen effects (produced in the conditions of photoexcitation of chlorine photosensitizers (PS)) with DNIC-TL effects. Our hopes that the concept of simultaneous PDT and DNIC-TL application is realizable rely on the “polymer effect” we found earlier – an increase of **specific** (per a PS molecule) photosensitizing activity in the photooxidation processes in the presence of amphiphilic polymers (AP) [27], that is achieved due to solubilization, a certain “encapsulation” of PS molecules. The latter factor may play a vital role in the manifestation of the DNIC-TL activity, namely, production of $NO^{\cdot}$ radicals. At the same time, AP, including ternary block-copolymers of ethylene- and propylene oxides – Pluronics - form weakly bound complexes with PS in the aqueous medium. Such complexes based on chlorine e6 and Pluronic were more active than the initial PPS in their photodynamic action on cell cultures and in the PDT treatment of wounds in laboratory animals [28,29].

As a model process, in which a photosensitizer activity in singlet oxygen generation was measured, we studied a standard reaction of photooxidation of an aminoacid substrate, tryptophan, in the aqueous medium, for different reaction mixture compositions, namely, for individual and combined applications of PS, DNIC-TL, Pluronic. When studying the mechanism of DNIC-TL decomposition in the photoexcitation conditions, one should take into account that DNIC-TL exist in mono- and dinuclear forms (M- and D-DNIC-TL), with D-DNIC-TL being diamagnetic, while M-DNIC-TL are identified by a characteristic EPR signal with the mean g-factor $g_m = 2.03$ [30]. According to Ref. [21], the differences in the biological activity of M-DNIC-TL and D-DNIC-TL forms are usually not discussed when considering the biomedical effects of DNIC-TL with thiol-containing ligands. The crucial role of D-DNIC-TL with glutathione is noted in the cytotoxic effect achievement, in particular, in the case of suppression of benign endometriosis in rats [31]. We will demonstrate below that, in the conditions of photosensitized oxidation of an organic substrate by molecular oxygen in the aqueous medium, the establishment of the determining effect on the mentioned process for only one of the two DNIC-TL forms, namely, D-DNIC-TL, does not represent a difficulty.

2. Material and methods

2.1. Kinetic studies

As a chlorine photosensitizer, we used N-methyl-di-D-glucamine salt of chlorin e6 (photoditazine, PD). As AP, Pluronic F127 (ternary block-copolymer of ethylene- and propylene oxide) was used, with M = 12600 Da and the ratio of propylene to ethylene units 65/200. DNIC-TL (Fig. 1) and S-nitrosoglutathione were synthesized by the method described in Ref. [32].

The EPR studies were conducted using a modified Radio-Pan radiospectrometer (Poland) at 77 K. The concentration of paramagnetic centers was calculated from the EPR signal intensity [30]. A frozen solution of DNIC-TL with cysteine with a known concentration was used as a standard. The complex was synthesized by the method described in Ref. [32].

Photooxidation of tryptophan (TP, analytical grade) was performed by molecular oxygen dissolved in water, in a quartz cuvette (with the reaction mixture volume of 3 $cm^3$and thickness $l = 1$ cm) at room temperature and stirring. The initial tryptophan concentration was $C_0^{TP} = 1.0{\cdot}10^{-5}$ M, photoditazine concentration was $C_0^{PD} = 1.5{\cdot}10^{-6}$ M. The DNIC-TL concentration was varied from $0.5{\cdot}10^{-5}$ to $5.4{\cdot}10^{-5}$ M, and the concentration of Pluronic F127 was varied from $5{\cdot}10^{-5}$ M to $5.0{\cdot}10^{-4}$ M, which essentially exceeded the critical micelle concentration, CMC $\sim 10^{-6}$ M. The irradiation of the reaction mixture was performed with an APS light diode (wavelength $\lambda = 400$ nm, power 86 mW, power flux density 3.6 mW/cm^2, sample illuminance 0.6 klx).

The photooxidation kinetics was followed via the decrease in the intensity of tryptophan photoluminescence ($\lambda_{ex} = 275$ nm,

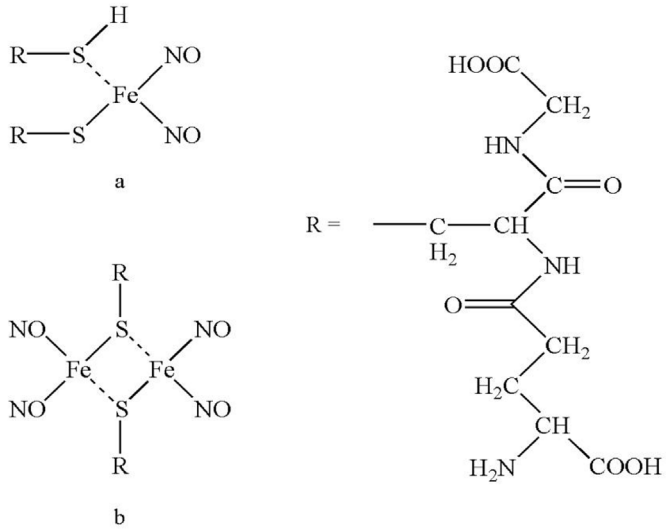

Fig. 1. Structural formulae of M-DNIC-TL (a) and D-DNIC-TL (b).

λ_{fl} = 355 nm). The luminescence spectra were acquired with a Cary Eclipse spectrofluorometer (Varian).

The kinetics of PD and D-DNIC-TL destruction was monitored via the decrease in the optical density of their UV absorption bands in the aqueous medium: λ = 655 nm (PD) and 310 nm (D-DNIC-TL). The kinetics of M-DNIC-TL photodestruction was followed via the decrease in the intensity of the characteristic EPR signal with the mean g-factor g_m = 2.03 [30].

UV-Vis absorption spectra of the solutions were acquired with a Cary 50 spectrophotometer (Varian).

The measurements of the observed rate constant k_{obs} of tryptophan photooxidation based on the conducted experiments were complicated by the fact that, with the light diode switch-on at the time point $t = 0$, not only tryptophan concentration $C^{TP}(t)$ in the reaction mixture decreased, but also concentrations $C^{PD}(t)$ and $C^{DNIC-TL}(t)$ of PD and DNIC-TL, respectively. Here, it should be noted that, according to the results of [26], photoinduced DNIC-TL decomposition with the release of $NO^{\cdot}$radicals, proceeding simultaneously with photosensitized tryptophan oxidation, may both initiate photodestruction of PS molecules and affect the rate of the target reaction – direct photooxidation of tryptophan.

Therefore, the equation for the kinetics of tryptophan photooxidation may be conveniently presented as follows:

$$\frac{dC^{TP}(t)}{dt} = -k^{TP}\cdot C^{TP}(t)c^{PD}(t)c^{DNIC-TL}(t), \tag{1}$$

Here k^{TP} is the constant of photosensitized tryptophan oxidation; $c^{PD}(t) \equiv C^{PD}(t)/C_0^{PD}$ and $c^{DNIC-TL}(t) \equiv C^{DNIC-TL}(t)/C_0^{DNIC-TL}$ are relative concentrations of PD and DNIC-TL, decreasing due to the degradation processes, thus, at $C^{TP}(0) \equiv C_0^{TP}$ one obtains:

$$C^{TP}(t) = C_0^{TP}\exp\left[-k^{TP}\int_0^t c^{PD}(\tau)c^{DNIC-TL}(\tau)d\tau\right]. \tag{2}$$

Further on, we will measure the observed rate constant k_{obs}^{TP} of tryptophan photooxidation by the decrease of tryptophan fluorescence, analyzing the linear part [0, Δt] of the corresponding kinetic dependence, during which about 20–30% of the tryptophan content in the initial solution is oxidized. Simultaneously, as follows from Eq. (2), the kinetics of PD and DNIC-TL destruction ought to be studied, i.e. the corresponding dependencies $c^{PD}(t)$ and $c^{DNIC-TL}(t)$. We will show below that, in the selected time interval [0, Δt] of tryptophan photooxidation and at the selected concentrations of all the participating components, the integral expression under the exponent (2) with the sufficient accuracy (~5%) may be presented in the form of a linear time dependence:

$$\chi_{TP}(\Delta t) \equiv \int_0^{\Delta t} c^{PD}(\tau)c^{DNIC-TL}(\tau)d\tau \approx \xi_{TP}\cdot\Delta t, \tag{3}$$

where ξ_{TP} is the interpolation kinetic parameter, and the kinetics of tryptophan oxidation over the mentioned time interval has a simple form:

$$\Delta C^{TP} \equiv C_0^{TP} - C^{TP}(\Delta t) = C_0^{TP}\cdot k^{TP}\xi_{TP}\Delta t. \tag{4}$$

Therefore, we present the rate constant k_{obs}^{TP} of tryptophan oxidation as follows, taking into account that the intensity of tryptophan photoluminescence $I(t)$ measured at the time point t is proportional to its current concentration $C^{TP}(t)$ in the working unit:

$$k_{obs}^{TP} = k^{TP}\xi_{TP} = \frac{\Delta I}{I_0\Delta t}, \tag{5}$$

where I_0 and ΔI are the initial intensity of tryptophan luminescence (in a.u.) and the change of this intensity due to photooxidation over the time Δt, respectively. The real rate constant of tryptophan oxidation in certain conditions is defined according to:

$$k^{TP} = k_{obs}^{TP}/\xi_{TP}, \tag{6}$$

implying that the value of ξ_{TP} is found numerically taking into account the individual conditions of tryptophan photooxidation. The effective rate constant k_{eff}^{TP} of tryptophan photooxidation per one PPS molecule may also be introduced, defined as $k_{eff}^{TP} = k^{TP}/C^{PD}$.

Since the efficiency of photosensitized oxidation of organic substrates by molecular oxygen in the presence of DNIC-TL may essentially depend on the rate of photoinduced degradation of both DNIC-TL and PD themselves, the corresponding rate constants k^{PD} and $k^{DNIC-TL}$ for PD and DNIC-TL photodestruction ought to be introduced, as well. It is natural to believe that k^{PD} will depend on the presence of DNIC-TL molecules in the solution, while $k^{DNIC-TL}$ will depend on the presence of PD. In these cases, we will calculate the mentioned rate constants k^{PD} and $k^{DNIC-TL}$ of photodestruction, based on the linear part of the corresponding kinetic plots according to:

$$\Delta C^{PD} \approx k^{PD}C_0^{PD}\xi_{PD}\Delta t, \quad \xi_{PD} = \frac{1}{\Delta t}\int_0^{\Delta t} c^{DNIC-TL}(t)dt, \tag{7a}$$

$$\Delta C^{DNIC} \approx k^{DNIC-TL}C_0^{DNIC-TL}\xi_{DNIC}\Delta t, \quad \xi_{DNIC} = \frac{1}{\Delta t}\int_0^{\Delta t} c^{PD}(t)dt, \tag{7b}$$

where $C_0^{(i)}$ and $\Delta C^{(i)}$ are concentration of ith component (PD, DNIC-TL) and the change in the concentration of the corresponding component over the time interval Δt, respectively; ξ_i is the interpolation kinetic parameter of ith component's degradation (PD or DNIC-TL), if the concentration of the other degrading component significantly changes in the process of degradation. As will be shown below, in the considered systems the detected degrees of conversion for the studied components over the time intervals admitting no higher than 5% deviations from the mentioned approximations, varied from 10-15%–50%.

2.2. Animal study

The animal studies were approved by the Local Ethical Committee of the Sechenov University (Moscow, Russia).

The experimental study of photoditazine (PD) combinations with DNIC-TL and Pluronic F127 was performed in 24 white male laboratory Wistar rats weighing 140–160 grams. The animals were obtained from the nursery of experimental animals at the Scientific Center for Biomedical Technologies of the Russian Academy of Sciences. In accordance with the European Convention (Strasbourg, 1986) and the Helsinki Declaration of the World Medical Association on the Humane Treatment of Animals (2000), all the animals were kept under standard vivarium conditions, 1 animal per cage, provided with a complex granulated feed and a constant access to water.

The model of a planar full-thickness wound was used in the studies [33–36]. The animals were anesthetized byan intramuscular injection of Zoletil 100 (Virbac S.A., Italy) solution, in the dose of 6 mg of the active ingredient per 1 kg of animal body weight, combined with Rometar (Spofa, Czech Republic), in the dose of 0.5 ml per 1 kg of animal body weight. In the interscapular space, a concentric skin flap with the subcutaneous tissue was excised up to the fascia propria (diameter ≈8–10 mm). A Teflon muff ring with an inner diameter of 20 mm was implanted into the created defect to ensure that the wound area was 300 mm^2 (Fig. 2).

All the 24 animals were divided into four study groups, depending on the method of the wound treatment (Table 1).

The studied drugs (dose - 1.0 ml) were injected into the soft tissues of the wound bottoms before photoactivation.

Photoactivation sessions with an AFS LED illumination device (Polironik, Russia, λ = 660 nm, power = 700 mW) started on the next day after the surgery. The wound was exposed to an unfocused beam for 1 min. This procedure was repeated on the third day after the operation.

On the fourth day after the initial operation, the animals were euthanized with an intraperitoneal injection of 2.0 ml of a 25% magnesium sulphate solution. This time point is considered optimal for

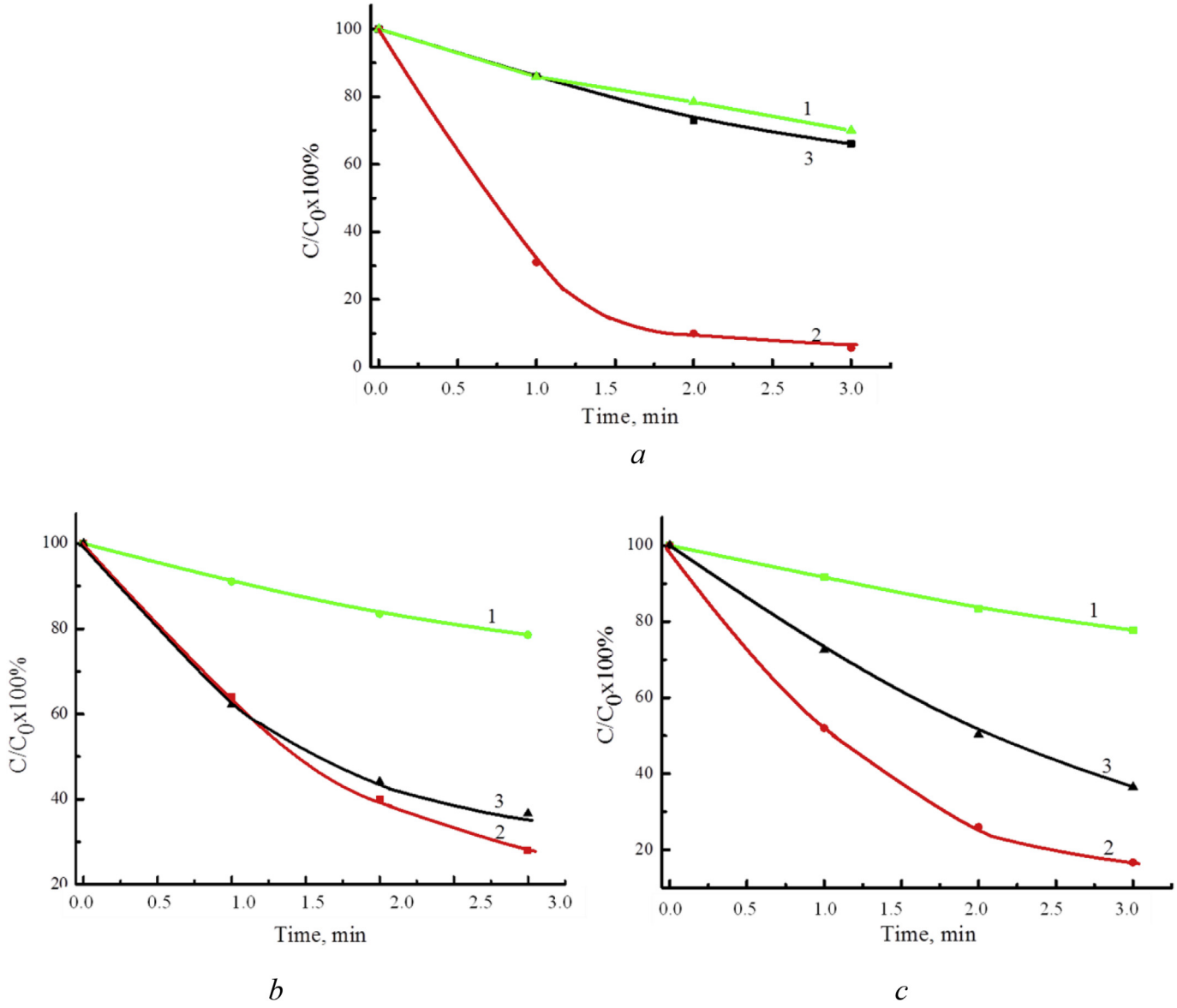

Fig. 2. Dependencies of the relative content on the duration of irradiation by the light with λ = 400 nm in aqueous solutions: di- and mononuclear DNIC forms (curves *1* and *2*, respectively) and PD (curve *3*), DNIC-TL in the absence of PD and PD in the DNIC-TL absence (*a*), DNIC-TL in the presence of PD and PD in the presence of DNIC-TL (*b*), DNIC-TL-PD systems in the presence of F127 (*c*). $C_0^{DNIC-TL} = 5.0 \cdot 10^{-5}$ M; $C_0^{PD} = 1.5 \cdot 10^{-6}$ M; $C_0^{F127} = 1.0 \cdot 10^{-4}$ M.

evaluation of both inflammatory and regenerative processes in skin wounds [33–36]. The muff rings were removed and the wound soft tissues were excised for a histological examination. The biological materials were fixed in 10% buffered neutral formalin for 24 h and poured with paraffin. 3 μm paraffin sections were stained with hematoxylin-eosin (H&E) and by Van Gieson method. The obtained microscopic preparations were studied using a LEICA DM4000 B LED universal microscope (Leica Microsystems, Germany) equipped with a LEICA DFC7000 T digital video camera (Leica Microsystems, Germany). The light microscopy studies were performed by two blinded pathologists.

A score system was applied to obtain the data on the morphological findings for a further semi-quantitative analysis. In each slide, the signs of inflammation (exudation, number of macro-phages), regeneration (vascularization, proliferation of fibroblasts, thickness and maturity of granulation tissue) and hemorrhagic reaction (erythrocyte extravasation) were scored on a 5-point scale (0 – not present, 1 – weak signs, 2 – moderate signs, 3 – intensive signs, 4 - maximum severity in the group).

The statistical analysis of the experimental data was performed with a GraphPad Prism version 7.00 for Windows (GraphPad Software, Inc.).

Table 1
The animal study design.

Study group	N	Wound treatment	Doses
Control 1	6	No treatment	
Control 2	6	DNIC-TL + hν	DNIC-TL solution – 0.013 mg/ml
Experimental 1	6	DNIC-TL-PD complex + hν	PD – 2 mg/ml, DNIC-TL – 0.013 mg/ml
Experimental 2	6	DNIC-TL-PD-F127 complex + hν	PD – 2мг/мл, DNIC-TL – 0.013 mg/ml, F127 – 20 mg/ml

The normal distribution of the quantitative data was checked by Shapiro-Wilk's normality test. The intergroup differences were analyzed by Kruskal-Wallis test followed by Dunn's multiple comparison test. The statistical analysis results were presented as column graphs of the mean values and SEM. The significant level of differences p was taken at a value < 0.05.

3. Results

As mentioned above, the general objective of this study is verifying a possibility to combine photodynamic effects on pathological tissues and simultaneous photoinitiaion of regulatory-regenerative processes in those tissues due to $NO^{\cdot}$ radicals generated by the decomposition of DNIC-TL. The obvious complexity of achieving such a solution is related to the fact that, in the conditions of photoexcitation, both processes – PDT and DNIC-TL decomposition – may be directed at the reciprocal suppression of their activity.

To reveal the details of such reciprocal effects and search for the factors which might minimize the potential mutual suppression of the two therapies, we first study model processes of degradation of DNIC-TL and a PS (photoditazine) under photoexcitation at $\lambda = 400$ nm. Additionally, in the considered aqueous system we introduce Pluronic F127, which has a significant effect on the kinetics of photosensitized oxidation of organic substrates in the PPS presence, as was already mentioned in Ref. [27]. It should be noted that irradiation of the systems under consideration with a light diode with $\lambda = 400$ nm did not influence the solubilizing activity of Pluronic F127.

3.1. Photodestruction of dinitrosyl iron complexes with thiol-containing ligands and PD under irradiation with the wavelength of $\lambda = 400$ nm

The dependencies of the relative content of di- and mononuclear DNIC-TL forms (curves *1* and *2*, respectively) in the absence of PD and the dependencies of the relative PD content (curve *3*) in the solution on the duration of irradiation in the absence of DNIC-TL are depicted in Fig. 2*a*. In Fig. 2*b*, similar dependencies of the relative content for both DNIC-TL types (curves *1* and *2*, respectively) and PD (curve *3*) are presented for aqueous DNIC-TL-PD mixtures. In Fig. 2*c*, the same type dependencies are shown for the relative content of mono- and dinuclear DNIC-TL forms (curves *1* and *2*, respectively) and PD (curve *3*) in a DNIC-TL-PD solution in the presence of Pluronic F127.

As follows from the presented data, DNIC-TL photolysis is accompanied by a sharp drop of the M-DNIC-TL concentration, i.e. of the number of paramagnetic centers in the solution (by 95%), while the D-DNIC-TL concentration calculated from the UV spectroscopy data decreases only by 32%. This finding indicates a significantly lower photoresistance of M-DNIC-TL as compared to that of D-DNIC-TL. As we mentioned above, when analyzing the kinetics of photodecomposition of DNIC-TL and PD, it is necessary to simultaneously detect the concentration changes of both components. Therefore, in the experiments, the results of which are displayed in Fig. 2, we measured the decrease of the PD concentration C^{PD} along with the decrease of the target component (DNIC-TL) concentration $C^{DNIC\text{-}TL}(t)$ due to photodegradation. In Fig. 3, the results of the numerical computations (dots) of the dependence $\chi_{D\text{-}DNIC\text{-}TL}(\Delta t) \approx \xi_{D\text{-}DNIC\text{-}TL} \times \Delta t$ are presented, obtained according to Eq. (7)*b*, and the corresponding interpolation linear approximations, determining the parameters $\xi_{D\text{-}DNIC\text{-}TL}$, which are used for the calculations of the rate constants of the considered D-DNIC-TL photodegradation based on Eq. (5) and Eq. (6). The corresponding parameters, as well as the correlation coefficients R^2 of those approximations are presented in Table 2. Similar dependencies for the calculations of the rate constants of D-DNIC-TL photodegradation in the PD-F127 presence and PD photodegradation in the D-DNIC-TL or D-DNIC-TL-F127 presence have also been obtained, and the corresponding rate constants and correlation coefficients R^2 are presented in Table 3.

As follows from the analysis of the totality of the presented data, the rate constant of M-DNIC-TL photodegradation exceeds the corresponding rate constant for D-DNIC-TL by almost an order of magnitude, thus, the regenerative properties of DNIC-TL [1] in the conditions of photoexcitation must be based on its dinuclear form. It should also be noted how important the contribution of the PS concentration changing due to photodegradation appears for the determination of the sought rate constants $k^{D\text{-}DNIC\text{-}TL}$, $k^{M\text{-}DNIC\text{-}TL}$ and k^{PD} based on the observed constants k^{i}_{obs} of the *i*th component (i.e. PPS or DNIC-TL), since this contribution affects the calculated parameter ξ_i based on the dependence in Fig. 3. Indeed, as follows from the data of Table 2, the photolysis rate constants of both DNIC-TL forms do not depend, within the error limits, on the presence of PPS and Pluronic F127 in the solution, while the corresponding estimations based on the observed constants k^{i}_{obs} with the contribution of the ξ_i factor appear erroneous. Apparently, when only DNIC-TL or only PD are present in the solution, $\xi_i = 1$ and $k^{i}_{obs} = k^{i}$. From the viewpoint of the discussed problem of the DNIC-TL effect on the photosensitizing activity of photoditazine, the obtained data indicate an increase of the rate constant k^{PD} of PD photodegradation by almost 3 times, likely caused by interaction of $NO^{\cdot}$radicals formed by DNIC-TL decomposition with the porphyrin base [37,38]. At the same time, the most important conclusion from the presented data is the establishment of an efficient “protective” role of Pluronic F127 in PS photodegradation, in the presence of which k^{PD} increased by “only 2 times” as compared to its initial value.

3.2. Photosensitized tryptophan oxidation in the reaction media containing DNIC-TL

First, we intend to discuss the data demonstrating how the rate constants k^{PD}_{TP} of PD decomposition change in the conditions of tryptophan oxidation. In Fig. 4, we present the plots of the corresponding rate constants k^{PD}_{TP} of PD photodestruction in the course of photosensitized tryptophan oxidation at $\lambda = 400$ nm vs. the concentration of Pluronic F127 at different DNIC-TL concentrations determined based on Eq. (7)*a*.

It follows from the dependencies displayed in Fig. 4 that the values of the rate constant k^{PD}_{TP} of PD photodestruction determined in the conditions of the proceeding reaction of tryptophan photooxidation, both in the presence of DNIC-TL and Pluronic and in their absence, appear lower than those for the corresponding rate constant k^{PD} (Table 2), obtained for the direct PD photolysis in the absence of tryptophan. In particular, in the absence of tryptophan and DNIC-TL in the system the rate constant of PD photodestruction $k^{PD} = 2.4 \times 10^{-3}$ s^{-1} (Table 2) is 2.4 times higher than the corresponding constant $k^{PD}_{TP} \approx 1 \times 10^{-3}$ s^{-1} in the presence of tryptophan. After the DNIC addition into the system, the differences between k^{PD} and k^{PD}_{TP} change only insignificantly, as follows from the comparison of the data in Table 2 and the plots presented in Fig. 5. The corresponding ratio reaches 4 in the absence of Pluronic F127 and equals 2.3 with the Pluronic present in the system. This finding indicates that singlet oxygen generated as a result of PPS photoexcitation is spent to a greater extent in the basic process of the substrate oxidation than in the PD photodestruction [39].

In Fig. 5, the dependencies of the efficient rate constant k^{TP}_{eff} of tryprophan oxidation on the Pluronic concentration C_0^{F127} are depicted for fixed DNIC-TL concentrations $C_0^{DNIC-TL}$. As the comparison of the profiles shows, Pluronic F127 present in the reaction medium in the concentration exceeding CMC not only promotes an increase of the rate constant of the organic substrate photooxidation, but also may boost the specific activity of DNIC-TL that is especially important for the photodynamic destruction of pathological cells and tissues in native systems. Thus, the presented dependencies answer positively the main question set in this study. Indeed, as follows from Fig. 5, in case of photosensitized oxidation of model organic substrates, it is possible to add DNIC-TL to the reaction medium while preserving acceptable rate constants of photosensitized oxidation. The dependencies displayed in

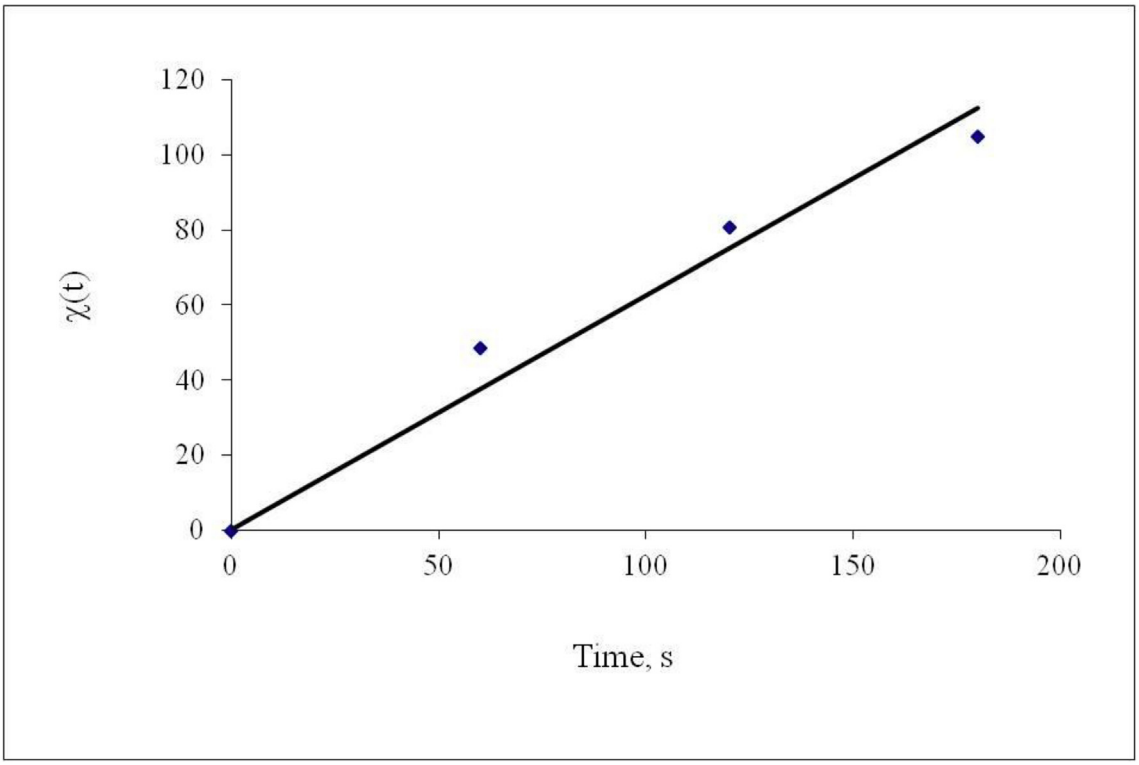

Fig. 3. Typical dependence $\chi_{D\text{-}DNIC\text{-}TL}(\Delta t) \approx \xi_{D\text{-}DNIC\text{-}TL} \times \Delta t$ (3*b*), plotted for the calculation of the parameters $\xi_{D\text{-}DNIC\text{-}TL}$, corresponding to the kinetic dependencies displayed in Fig. 2 (*a, b*) for aqueous solutions of DNIC-TL-PD.

Fig. 5, in fact, generally reflect the interrelations of the reaction mixtures' components, which may be formed for PDT procedures. In doing so, one may base upon the possibility found in this study, namely, the initiation of additional effects, both cytotoxic and regulatory-regenerative (determined by addition of DNIC-TL) simultaneously with the photosensitizing action on pathological fragments of diseased tissues [38].

In connection with the dependencies presented in Fig. 5, one additional remark should be made. Since, in the course of photoinduced DNIC-TL decomposition with the release of *NO·* radicals in the reaction medium, not only photodestruction of PS molecules occurs, but also the rate of the direct tryptophan oxidation upon interaction with *NO·* may increase, the problem of increasing the integral rate of this process should consist in the exclusion or essential reduction of the *NO·* negative destructive action on PS molecules with the simultaneous preservation of the PS action on tryptophan. We have shown with additional experiments that tryptophan in not oxidized upon DNIC photoexcitation, thus, we believe that *NO·* does not participate in the substrate oxidation. The dependencies in Fig. 5 indicate a principal possibility of this problem solution due to addition of Pluronic F127 to the reaction medium. As mentioned above, the key role of Pluronic in this case is determined by the phenomenon we found earlier - formation of PS-AP complexes resulting in the photosensitizer solubilization. Such solubilization facilitates not only deaggregation of PS molecules thus leading to the increase of the photooxidation rate constant [40], but also efficient protection of PS (PD) molecules via their shielding from the action of *NO·* radicals formed upon DNIC-TL photodecomposition.

Table 3
Calculated parameters ξ and R^2 and rate constants of PD decomposition (direct photolysis), for different compositions of the reaction system. The integral relative error for the presented rate constants of PD photolysis does not exceed 10%.

Aqueous solution	ξ_i	R^2	k_{obs}^{PD} $\times 10^3$, s^{-1}	k^{PD} $\times 10^3$, s^{-1}
PD	1.0	–	2.4	2.4
DNIC-TL-PD	0.895	0.998	6.3	7.0
DNIC-TL-PD-F127	0.896	0.998	4.2	4.7

3.3. Histological studies

A series of experiments on the treatment of model (planar full-thickness) wounds in rats, with the simultaneous application of PDT and dinitrosyl iron complexes, was conducted. As a photosensitizer, we used photoditazine in the presence and absence of Pluronic F127.

In the Control 1 group, the wound bottom was lined with a fibrin clot, covering a layer of immature granulation tissue. This tissue

Table 2
Calculated parameters ξ and R^2 and rate constants of D-DNIC-TL and M-DNIC-TL decompostion, for different compositions of the reaction medium. The integral relative errors for the presented rate constants of D-DNIC-TL and M-DNIC-TL photolysis do not exceed 10% and 20%, respectively.

Aqueous solution	ξ_i	R^2	k_{obs}^{D-DNIC} $\times 10^3$, s^{-1}	$k^{D\text{-}DNIC\text{-}TL} \times 10^3$, s^{-1}	k_{obs}^{M-DNIC} $\times 10^3$, s^{-1}	$k^{M\text{-}DNIC\text{-}TL} \times 10^3$, s^{-1}
DNIC-TL	1.0	–	2.0	2.0	11.4	11.4
DNIC-TL-PD	0.624	0.965	1.4	2,2	6.0	9.6
DNIC-TL-PD-F127	0.682	0.969	1.4	2.0	8.0	11.7

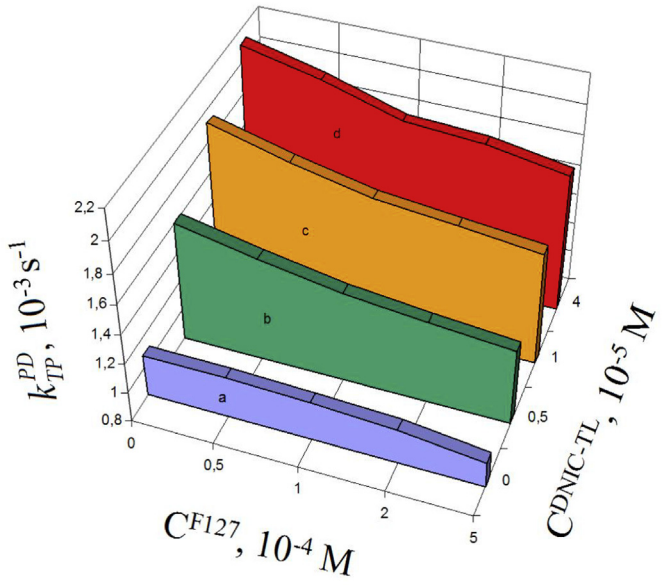

Fig. 4. Profiles of the effective rate constant k_{TP}^{PD} of PD photodestruction ($C_0^{PD} = 1.5 \times 10^{-6}$ M) at λ = 400 nm in the course of photosensitized tryptophan oxidation plotted vs. the Pluronic concentration, at different DNIC –TL concentrations. The profiles correspond to the following concentrations $C_0^{DNIC-TL}$: *a* - 0; *b* - 5×10^{-6} M; *c* - 1.0×10^{-5} M; *d* - 4.0×10^{-5} M.

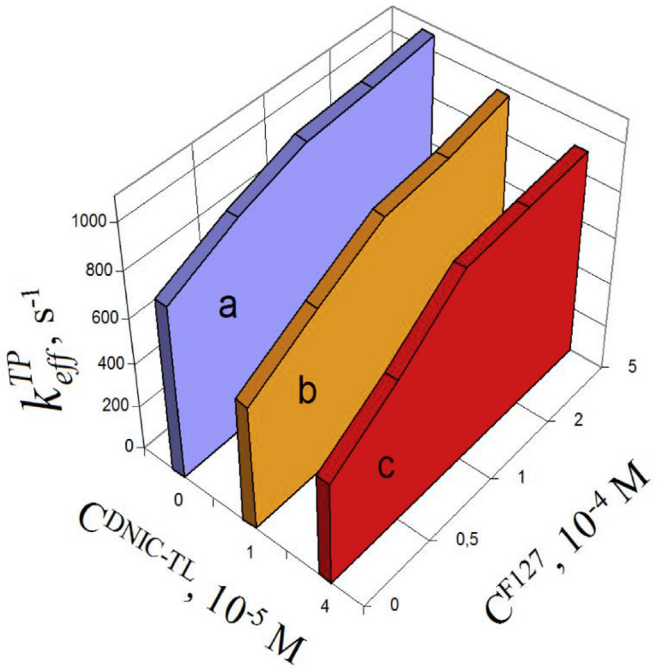

Fig. 5. Profiles of the effective rate constant k_{eff}^{TP} of tryptophan photooxidation vs. the Pluronic F127 concentration, at different DNIC-TL concentrations. ($C_0^{PD} = 1.5 \times 10^{-6}$ M, $C_0^{TP} = 1.5 \times 10^{-6}$ M). The profiles correspond to the following concentrations C_0^{DNIC}: *a* - 0; *b* - 1.0×10^{-5} M; *c* - 4.0×10^{-5} M.

consisted of rare multidirectional groups of fibroblasts, numerous macrophages, lymphocytes and neutrophilic leukocytes, as well as infrequent newly formed capillary vessels and very thin collagen fibers in the extracellular matrix. In addition to inflammatory infiltration, there were edema, hyperemia and stasis of erythrocytes in the micro-circulatory vessels (Fig. 6a, Fig. 7).

In the Control 2 group (DNIC-TL + hν), the wound bottom was lined with a thinner clot of fibrin, containing fewer neutrophilic leukocytes than in Control 1 ($p = 0.1176$). In most animals (5 out of 6) we observed a greater volume and higher maturity of granulation tissue (125% more mature, $p < 0.0001$) with enhanced proliferation of fibroblasts (77% higher, $p = 0.0007$). Multiple vertically oriented blood vessel strands were partially differentiated into venules and arterioles. Inflammatory infiltration was relatively low (Figs. 6b and 7).

In the Experimental group 1 (DNIC-TL-PD complex + hν), the fibrin clot at the wound bottom was thinner than that in Control 1 (55% less exudation, $p = 0.0112$) and partially organized by fibroblasts. The underlying granulation tissue had the same volume and maturity as those in the previous group. Inflammatory infiltration was reduced in comparison with the previous group. Strands of fibroblasts remained irregular in some areas, while they tended to have a longitudinal orientation at other sites. The tissue contained relatively many macrophages (59%, a higher amount than that in Control 1, $p = 0.0154$) and lymphocytes, but neutrophils were mostly absent. Some fibroblasts were in the mitotic state. Most animals' blood vessels were full of red blood cells and surrounded by areas of erythrocyte extravasation (Figs. 6c and 7).

In the Experimental group 2 (DNIC-TL-PD-F127 complex + hν), the fibrin clot was the thinnest among all groups (70% weaker exudation than that in Control 1, $p = 0.0006$) and was partially organized by underlying fibroblasts (Figs. 6d and 7). This granulation tissue occupied the largest volume in comparison with all the other groups (187% more mature than that in Control 1, $p < 0.0001$). Very pronounced signs of fibroblast proliferation (155% higher than that in Control 1, $p < 0.0001$) correlated with a high cellular density in these areas. The number of cells in the state of mitosis was increased. Inflammation was very weak. In comparison with the Experimental group 1, this study group lacked hemorrhages (79% less signs of erythrocyte extravasation, $p = 0.0002$), they were small in size and were revealed only in 2 out of 6 animals.

The histological analysis of rat wound tissues revealed a reliably marked acceleration of wound healing after the application of DNIC-TL per se with the subsequent photoactivation in comparison with the control group without treatment. The fibrin clot lining the wound surface was thinner, inflammation was inhibited and the granulation tissue became larger and more mature. These results are consistent with our previous research [34]. There were no significant differences in wound healing between laboratory animals in this group and the DNIC-TL-PD complex + hν experimental group. Nevertheless, the rats in the latter group had more frequent erythrocyte extravasation, which was associated with the effect of PD on the permeability of microcirculatory blood vessel walls [36].

The most beneficial effects were observed after the application of DNIC-TL-PD-F127 complex + hν. Inflammation was reduced to the minimum and the granulation tissue occupied the largest volume and was the most mature among all the study groups. At the same time, manifestations of vascular permeability decreased sharply. This supports the study results mentioned above concerning the blood vessel endothelium preservation effect of Pluronic F127 against the PD-mediated photodestruction.

We believe that the results of this study open new opportunities in antimicrobial photodynamic therapy, since they uncover the conditions in which the application of photosensitizers in the solubilized state (provided by polymer surfactants, in particular, Pluronic F127) efficient in the treatment of complicated wounds [28] may be combined with the application of DNIC-TL-PD without the loss of the PDT efficiency.

Competing interests statement

Authors declare no competing interests.

Acknowledgements

This study was financially supported by the Russian Science Foundation (Grant No.16-13-10295).

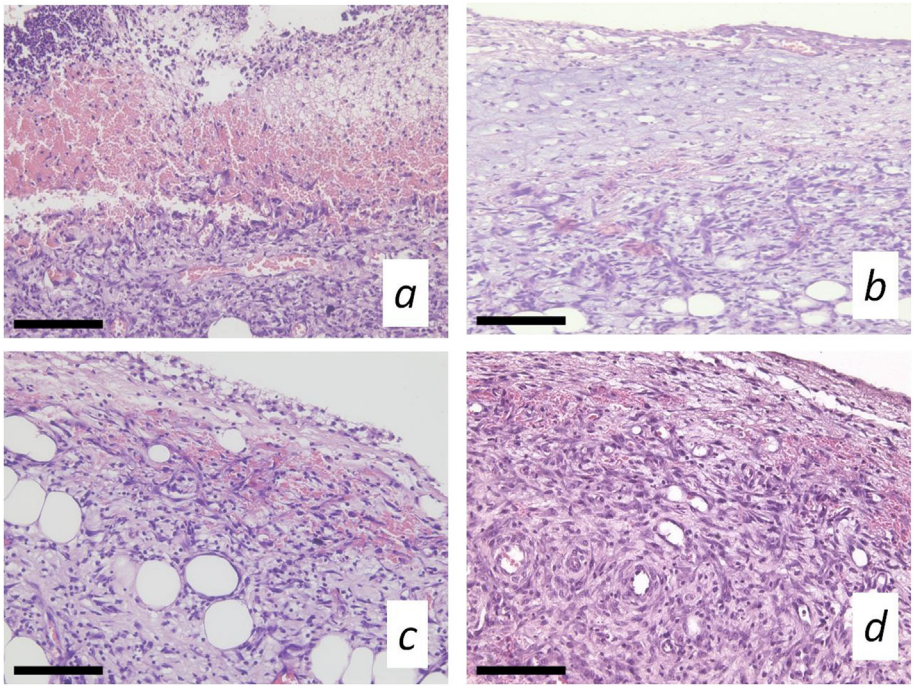

Fig. 6. Histological slides of wound tissues in the control (A, B) and experimental (C, D) groups after two photoactivation sessions, H&E staining, magnification 200 × , Bar = 50 μm.
a – Control 1: fibrin clot with granulation tissue underneath it, containing fibroblasts, lymphocytes, macrophages, neutrophils and blood vessels, H&E staining. b – Control 2: maturing granulation tissue with vertically oriented capillaries. c – Experimental 1: erythrocyte extravasation in granulation tissue. d – Experimental 2: mature granulation tissue with intensive fibroblast proliferation and excessive number of arterioles and capillaries, thin exudative layer on the wound surface.

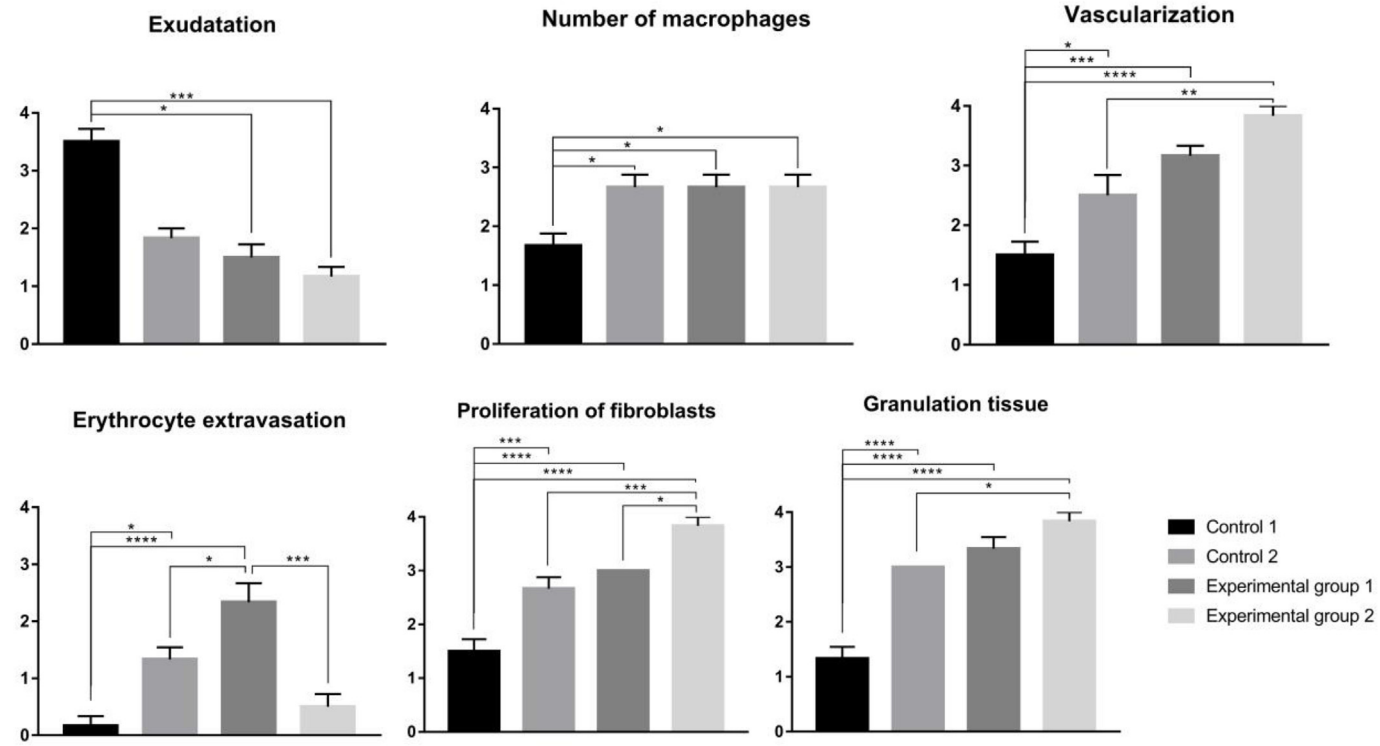

Fig. 7. Statistical analysis of morphological findings, Kruskal-Wallis test followed by Dunn's multiple comparison test, * - $p < 0.05$, ** - $p < 0.01$, *** - $p < 0.001$, **** - $p < 0.0001$.

References

[1] A.F. Vanin, Dinitrosyl Iron Complexes with Thiol-containing Ligands: Physical Chemistry, Biology, Medicine, Moscow-Izhevsk, 2015, p. 219.
[2] A.F. Vanin, Nitric oxide and its detection in biosystems by electron paramagnetic resonance, Physics–Uspekhi 170 (2000) 455–458.
[3] F. Murad, Discovery of some of the biological effects of nitric oxide and its role in cell signaling, Biosci. Rep. 19 (1999) 133–154.
[4] L.A.J. Mur, T.W. Carver, E. Prats, NO way to live; the various roles of nitric oxide in plant-pathogen interactions, J. Exp. Bot. 57 (2006) 489–505.
[5] A. Besson-Bard, A. Pugin, D. Wendehenne, New insights into nitric oxide signaling in plants, Annu. Rev. Plant Biol. 59 (2008) 21–39.
[6] D.A. Wink, J.B. Mitchell, Chemical biology of nitric oxide: insights into regulatory, cytotoxic, and cytoprotective mechanisms of nitric oxide, Free Radic. Biol. Med. 25 (1998) 434–456.
[7] B. Muller, A.L. Klechev, J.L. Alencar, A.F. Vanin, J.-C. Stoclet, Ann. N-Y. Acad. Sci. 962 (2002) 131–139.
[8] C.M. Boulanger, Secondary endothelial dysfunction: hypertension and heart failure, J. Mol. Cell. Cardiol. 31 (1999) 39–49.
[9] H. Drexler, Nitric oxide and coronary endothelial dysfunction in humans, Cardiovasc. Res. 43 (1999) 572–579.

[10] V.J. Thannickal, B.L. Fanburg, Reactive oxygen species in cell signaling, Am. J. Physiol. Lung Cell Mol. Physiol. 279 (2000) 1005–1028.
[11] M. Sheldon, Reactive oxygen species: toxic molecules or spark of life? Crit. Care 10 (2006) 208.
[12] I. Petrushanko, N. Bogdanov, E. Bulygina, B. Grenacher, T. Leinsoo, A. Boldyrev, M. Gassmann, A. Bogdanova, Na-K-ATPase in rat cerebellar granule cells is redox sensitive, Am. J. Physiol. Regul. Integr. Comp. Physiol. 290 (2006) 916–925.
[13] A. Petry, M. Weitnauer, A. Görlac, Receptor activation of NADPH oxidases, Antioxidants Redox Signal. 13 (2010) 467–487.
[14] V.J. Thannickal, B.L. Fanburg, Reactive oxygen species in cell signaling, Am. J. Physiol. Lung Cell Mol. Physiol. 279 (2000) L1005–L1028.
[15] K. Apel, H. Hirt, Reactive oxygen species: metabolism, oxidative stress, and signal transduction, Annu. Rev. Plant Biol. 55 (2004) 373–399.
[16] H. Nakamura, K. Nakamura, J. Yodoi, Redox regulation of cellular activation, Ann. Rev. Immunol. 15 (1997) 351–369.
[17] Y. Kovtun, W.L. Chiu, G. Tena, J. Sheen, From the cover: functional analysis of oxidative stress-activated mitogen-activated protein kinase cascade in plants, Proc. Nat. Acad. Sci. USA. 97 (2000) 2940–2945.
[18] J.J. Poderoso, M.C. Carreras, C. Lisdero, N. Riobo, et al., Nitric oxide inhibits electron transfer and increases superoxide radical production in ratheart mitochondria and submitochondrial particles, Arch. Biochem. Biophys. 328 (1996) 85–92.
[19] C.X.C. Santos, N. Anilkumar, M. Zhang, A.C. Brewer, A.M. Shah, Redox signaling in cardiac myocytes, Free Radic. Biol. Med. 50 (2011) 777–793.
[20] J. Murray, S.W. Taylor, B. Zhang, S.S. Ghosh, R.A. Capaldi, Oxidative damage to mitochondrial complex I due to peroxynitrite, J. Biol. Chem. 278 (2003) 37223–37230.
[21] E.N. Bugrova, N.A. Tkachev, L.V. Adamyan, Y.D. Mikoyan, O.V. Paklina, A.A. Stepanyan, A.F. Vanin, Dinitrosyl iron complexes with glutation suppress experimental endometriosis in rats, Eur. J. Pharmacol. 727 (2014) 140–147.
[22] Nitrosation Reactions and the Chemistry of Nitric Oxide by D.L.H. Williams, Elsevier BV, Amsterdam, 2004, pp. 139–140.
[23] R.J. Singh, N. Hogg, J. Joseph, B. Kalyanaraman, Photosensitized decomposition of S-nitrosothiols and 2-methyl-2-nitrosopropane. Possible use for site-directed nitric oxide production, FEBS (Fed. Eur. Biochem. Soc.) Lett. 360 (1995) 47–51.
[24] P. Singh, E.F. Ulman, Nitroso compounds and AZo dioxidees as quenchers of singlet oxygen ($^1\Delta_2$) and sensitizer triplet states, J. Am. Chem. Soc. 98 (1976) 3018–3019.
[25] Y.L. Chow, J.N.S. Tam, K.S. Pillay, Photoreactions of nitroso compounds in solution.' XXIV. Photooxidation and photodecomposition of C-nitroso compounds, Can. J. Chem. 50 (1972) 1044–1050.
[26] J.A. Maassen, Th.J. de Boer, C-Nitroso compounds. Part XXVI: photochemistry of C-nitroso compounds. The photooxidation of ethylbenzene in the presence of 2-methyl-2-nitrosopropane, Recl. Trav. Chim. Pays-Bas 92 (2010) 185–194.
[27] N.A. Aksenova, T. Oles, T. Sarna, N.N. Glagolev, A.V. Chernjak, V.I. Volkov, S.L. Kotova, N.S. Melik-Nubarov, A.B. Solovieva, Development of novel formulations for photodynamic therapy on the basis of amphiphilic polymers and porphyrin photosensitizers. Porphyrin-polymer complexes in model photosensitized processes, Laser Phys. (2012) 1642–1649.
[28] T.M. Zhiyentayev, U.T. Boltaev, A.B. Solov'eva, N.A. Aksenova, N.N. Glagolev, A.V. Chernjak, N.S. Melik-Nubarov, Complexes of chlorin e6 with pluronics and polyvinylpyrrolidone: structure and photodynamic activity in cell culture, Photochem. Photobiol. 90 (2014) 171–182.
[29] T.G. Rudenko, A.B. Shekhter, A.E. Guller, N.A. Aksenova, N.N. Glagolev, A.V. Ivanov, R.K. Aboyants, S.L. Kotova, A.B. Solovieva, Specific features of the wound healing process occurring against the background of phootodynamic therapy using fotoditazin photosensitizer-amphiphilic polymer complexes, Photochem. Photobiol. B. 90 (2014) 1413–1422.
[30] A.F. Vanin, A.P. Poltorakov, V.D. Mikoyan, L.M. Kubina, D.Sh. Burbaev, V.O. Shvydkiy, Polynuclear water-soluble dinitrisyl iron complexes with cysteine or glutathione ligands: electron paramagnetic resonance and optical studies, Nitric Oxide Biol. Chem. 23 (2010) 136–149.
[31] E.N. Bugrova, N.A. Tkachev, L.V. Adamyan, V.D. Mikoyan, O.V. Paklina, A.A. Stepanyan, A.F. Vanin, Dinitrosyl ion complexes with glutathione suppressexperimental endometriosis in rats, E. J. Pharmacol. 727 (2014) 140–147.
[32] R.R. Borodulin, L.N. Kubrina, V.D. Mikoyan, A.P. Poltorakov, V.A. Serezhenkov, E.R. Yakhontova, A.F. Vanin, Dinitrosyl iron complexes with glutathione as NO and NO^- donors, Nitric Oxide Biol. Chem. 29 (2013) 4–6.
[33] A.B. Shekhter, T.G. Rudenko, V.A. Serezhenkov, A.F. Vanin, A.V. Pekshev, Beneficial effect of gaseous nitric oxide on the healing of skin wounds, Nitric Oxide 12 (2005) 210–219.
[34] A.B. Shekhter, T.G. Rudenko, V.A. Serezhenkov, A.F. Vanin, Dinitrosyl iron complexes with thiol ligands promote skin wound healing in animals, Biophysics 52 (2007) 515–520.
[35] A.B. Shekhter, T.G. Rudenko, L.P. Istranov, A.E. Guller, R.R. Borodulin, A.F. Vanin, Dinitrosyl iron complexes with glutathione incorporated into a collagen matrix as a base for the design of drugs accelerating skin wound healing, Eur. J. Pharm. Sci. 78 (2015) 8–18.
[36] T.G. Rudenko, A.B. Shekhter, A.E. Guller, N.A. Aksenova, N.N. Glagolev, A.V. Ivanov, R.K. Aboyants, S.L. Kotova, A.B. Solovieva, Specific features of the early stage of the wound healing process occurring against the background of photodynamic therapy using fotoditazin photosensitizer-amphiphilic polymer complexes, Photochem. Photobiol. 90 (2014) 1413–1422.
[37] C.L. Conrado, J.L. Bourassa, C. Egler, S. Wecksler, P.C. Ford, Photochemical investigation of Roussin's red salt Esters, Inorg. Chem. 42 (2003) 2288–2293.
[38] A.F. Vanin, D. Svistunenko, V.D. Mikoyan, et al., Endogenous superoxide production and the nitrite/nitrate ratio control the concentration of bioavailable free nitric oxide in leaves, J. Biol. Chem. 279 (2004) 24100.
[39] N.A. Kuznetsova, O.L. Kaliya, Oxidative photobleaching of phthalocyanines in solution, J. Porphyr. Phthalocyanines 16 (2012) 705–712.
[40] A.B. Solovieva, N.S. Melik-Nubarov, T.M. Zhiyentayev, P.I. Tolstih, I.I. Kuleshov, N.A. Aksenova, E.A. Litmanovich, N.N. Glagolev, V.A. Timofeeva, A.V. Ivanov, Development of novel formulations for photodynamic therapy on the basis of amphiphilic polymers and porphyrin photosensitizers. Pluronic influence on photocatalytic activity of porphyrins, Laser Phys. 19 (2009) 1–8.